Numerical Investigation on Drag Reduction Effect by Mass Injection from Porous Boundary Wall

Zhao Yong(赵勇)[1,2], *Gao Yun*(高云)[3*], *Jiang Zongyu*(姜宗玉)[4], *Wang Tianlin*(王天霖)[1], *Zou Li*(邹丽)[5]

1. Transportation Equipment and Ocean Engineering College, Dalian Maritime University, Dalian 116026, P. R. China;
2. State Key Laboratory of Ocean Engineering, Shanghai Jiao Tong University, Shanghai 200240, P. R. China;
3. State Key Laboratory of Oil and Gas Reservoir Geology and Exploration, Southwest Petroleum University, Chengdu 610500, P. R. China;
4. Wood Group Mustang, Shanghai 201206, P. R. China;
5. School of Naval Architecture, Dalian University of Technology, Dalian 116024, P. R. China

(Received 30 September 2014; revised 7 April 2015; accepted 12 April 2015)

Abstract: Interaction between the injected flow from the porous wall and the main flow can reduce drag effectively. The phenomenon is significant to the flight vehicle design. The intensive flux of injection enhances difficulty of numerical simulation and requires higher demands on the turbulence model. A turbulent boundary layer flow with mass injection through a porous wall governed by Reynolds averaged Navier-Stokers (RANS) equations is solved by using the Wilcox's k-ω turbulence model and the obtained resistance coefficient agrees well with the experimental data. The results with and without mass injection are compared with other conditions unchanged. Velocity profile, turbulent kinetic energy and turbulent eddy viscosity are studied in these two cases. Results confirm that the boundary layer is blowing up and the turbulence is better developed with the aid of mass injection, which may explain the drag reduction theoretically. This numerical simulation may deepen our comprehension on this complex flow.

Key words: mass injection; boundary layer blowing up; drag reduction; turbulence model; Reyndds averaged Navier-Stokers (RANS)

CLC number: O35 **Document code**: A **Article ID**: 1005-1120(2015)02-0250-05

0 Introduction

Flows through porous wall with mass injection, or termed as blowing, are encountered in many engineering applications such as boundary layer controlling, transpiration cooling and resistance reducing[1-3]. The mass injection can impressively reduce resistance experienced by turbulent flow in pipes, and drag encountered by ships and airplanes, as well as the efficiency losses of turbines and turbo compressors[4-5]. Thus turbulent boundary layer flow with mass injection has great engineering significance. Since the prediction of the effects of mass injection on slender aerodynamic body is of technological interest, several studies of boundary layers with mass injection have been carried out [6-7]. An interesting aspect of the study of flows with mass injection is the phenomenon of boundary layer blow off[5]. When the additional fluid is injected into a boundary layer, the injected fluid simply fills the region near the wall and significantly alters profiles of the flow variables. Due to the integration of the fluids near the wall, usual methods for handling two-point boundary conditions would become invalid, especially when the blowing parameter is large[8].

* **Corresponding author**: Gao Yun, Lecturer, E-mail: dutgaoyun@163.com.

How to cite this article: Zhao Yong, Gao Yun, Jiang Zongyu, et al. Numerical investigation on drag reduction effect by mass injection from porous boundary wall [J]. Trans. Nanjing U. Aero. Astro., 2015,32(2):250-254.
http://dx.doi.org/10.16356/j.1005-1120.2015.02.250

This failure can be attributed to poor convergence and instabilities of the numerical methods[9].

Generally, the problem of porous wall with mass addition needs more attention to the drag reduction effect in engineering application, and on the other aspect, to understand the behavior of such complex flow. The simplest case is a turbulent boundary layer occurring on a flat plate at zero incidences. This flow model is, however, of great practical importance and it can be used in the calculation of the frictional resistance on ships, lifting surfaces, the blades of turbines and rotary compressors[6]. Therefore, numerical work is taken to investigate the two-dimensional turbulent boundary layer flow over a smooth and permeable flat surface with mass injection.

1 Equations and Turbulence Model

Two-dimensional steady and incompressible boundary layer flow is governed by

$$\frac{\partial U}{\partial x}+\frac{\partial V}{\partial y}=0 \tag{1}$$

$$U\frac{\partial U}{\partial x}+V\frac{\partial U}{\partial y}=-\frac{1}{\rho}\frac{\mathrm{d}p}{\mathrm{d}x}+\frac{\partial}{\partial y}\left[(\nu+\nu_{\mathrm{T}})\frac{\partial U}{\partial y}\right] \tag{2}$$

where U, V are the stream-wise and normal averaged velocity components; ρ, P the fluid density and pressure; ν, ν_{T} the molecular and turbulent eddy kinetic viscosity.

Kolmogorov and Saffman creatively and independently developed the k-ω model. Wilcox has continually refined and improved the model during the past three decades and demonstrated its accuracy for a wide range of turbulent flows [10-12]. Here the latest version of k-ω model[12] is chosen, which considers the turbulent eddy viscosity[12] as follows

$$\nu_{\mathrm{T}}=k/\tilde{\omega},\tilde{\omega}=\max\left(\omega,\frac{7}{8}\sqrt{\frac{2S_{ij}S_{ij}}{\beta^{*}}}\right) \tag{3}$$

Reynolds stress for incompressible flow is

$$\tau_{ij}=2\rho\nu_{\mathrm{T}}S_{ij} \tag{4}$$

Turbulence kinetic energy equation is

$$U_j\frac{\partial k}{\partial x_j}=\tau_{ij}\frac{\partial U_i}{\partial x_j}-\beta^{*}k\omega+\frac{\partial}{\partial x_j}\left[\left(\nu+\sigma^{*}\frac{k}{w}\right)\frac{\partial k}{\partial x_j}\right] \tag{5}$$

Specific dissipation rate is

$$U_j\frac{\partial \omega}{\partial x_j}=\alpha\frac{\omega}{k}\tau_{ij}\frac{\partial U_i}{\partial x_j}-\beta\omega^{2}+\frac{\sigma_d}{\omega}\frac{\partial k}{\partial x_j}\frac{\partial \omega}{\partial x_j}+\frac{\partial}{\partial x_j}\left[\left(\nu+\sigma\frac{k}{\omega}\right)\frac{\partial \omega}{\partial x_j}\right] \tag{6}$$

Closure coefficients and auxiliary relations are

$$\alpha=\frac{13}{25},\ \beta=\beta_0 f_\beta,\ \beta^{*}=\frac{9}{100}$$
$$\sigma=\frac{1}{2},\ \sigma^{*}=\frac{3}{5},\ \sigma_d=\frac{1}{8} \tag{7}$$

$$\sigma_d=\begin{cases}0, & \dfrac{\partial k}{\partial x_j}\dfrac{\partial \omega}{\partial x_j}\leqslant 0\\ \sigma_d, & \dfrac{\partial k}{\partial x_j}\dfrac{\partial \omega}{\partial x_j}>0\end{cases} \tag{8}$$

$$\beta_0=0.070\ 8,\quad f_\beta=\frac{1+85\chi_\omega}{1+100\chi_\omega},\quad \chi_\omega\equiv\left|\frac{\Omega_{ij}\Omega_{jk}S_{ki}}{(\beta^{*}\omega)^{3}}\right| \tag{9}$$

where

$$\Omega_{ij}=\frac{1}{2}\left(\frac{\partial U_i}{\partial x_j}-\frac{\partial U_j}{\partial x_i}\right),S_{ij}=\frac{1}{2}\left(\frac{\partial U_i}{\partial x_j}+\frac{\partial U_j}{\partial x_i}\right) \tag{10}$$

It can be easily verified that the quantity χ_ω is zero for two-dimensional flows. In the porous wall, the boundary condition is

$$U=0,\quad V=V_{\mathrm{w}} \tag{11}$$

On the contrary, the boundary condition of solid wall is non-slip, i. e.

$$U=0,\quad V=0 \tag{12}$$

For the model equation, the boundary condition is specified as

$$k=0,\quad \omega=\frac{6\nu_{\mathrm{w}}}{\beta_0 d^{2}} \tag{13}$$

where d is the distance of the nearest grid to the wall.

2 Numerical Test

2.1 Flow parameter

The flow parameters in the numerical calculation are listed in the following. Surface mass flux $\dot{m}=\rho_{\mathrm{w}}V_{\mathrm{w}}$ is constant as 0.042 97 kg/(m^2 · s), where ρ_{w} is the transpired air density and V_{w} the normal velocity from the porous wall; Free stream air velocity U_∞ is 9.397 m/s. Both the transpired and free stream air temperature T, density ρ and pressure P are 297.8 K, 1.193 kg/m^3, 101 984 Pa, respectively. The schematic diagram of boundary layer with mass injection is shown in Fig. 1. Air viscosity coefficient ν is

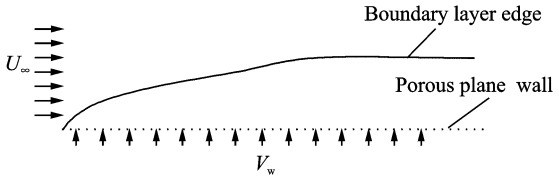

Fig. 1 Boundary layer with mass injection

1.458×10^{-6}, the length of the flat $L=5$ m, and the Reynolds number based on the free stream air velocity and flat length is 3.23×10^{7}.

These parameters are the same as those in the experiment conducted by Andersen[13]. His work measured resistance coefficient along the flat. Hence, the measured resistance coefficient can be used to validate our numerical calculation. The coefficient is defined by $C_f=2\tau_w/\rho U_\infty^2$, where $\tau_w=\rho\nu_T\partial U/\partial y\,|_{y=0}$. This physical quantity is determined by the derivative of velocity and eddy viscosity, so it is an appropriate candidate for checking numerical simulation.

2.2 Numerical method and mesh convergence validation

On the basis of laminar flow, we supplement codes of Wilcox′s k-ω model[12] to calculate the flow. Iterative algorithm is used to solve the equations, in the sequence of momentum equations, continuous equation and turbulence model equations. In the discrete equations, the second-order upwind difference scheme is used for the convection term. The others are calculated by using the second-order central difference scheme. Uniform incoming velocity, free outflow, no-slip wall and zero normal gradient are defined for the boundary conditions, respectively. In order to check the convergence of meshes, three nested grids with nodes number of 301×101, 151×51, 75×25 are used to discrete the computational zone with the dimension of 5 m×0.12 m. The frictional resistance coefficient along the plate is shown in Fig. 2. It is shown that the numerical results are independent of the grid density. In the following calculation, the middle density grid, 151×51, is selected.

Local frictional coefficient is compared with the experimental result, as shown in Fig. 3. The

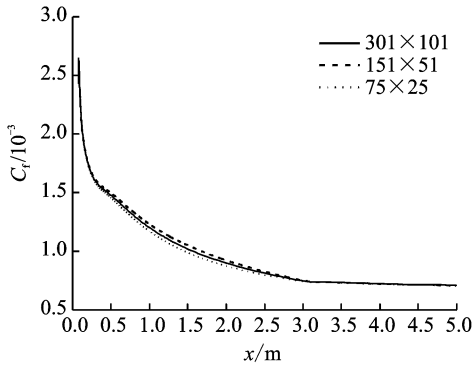

Fig. 2 Comparison of local frictional coefficient along the plate with three mesh density

numerical result is very close to the experimental result[13], especially in the latter part of the wall. It clearly indicates the high precision of the numerical method. Therefore, Wilcox′s k-ω model[12] is suitable for turbulent boundary calculation with mass injection.

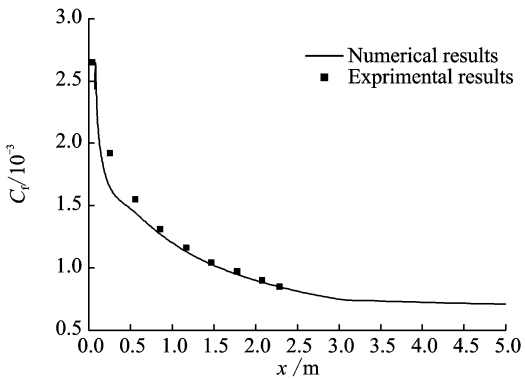

Fig. 3 Comparison of local frictional coefficient along the plate between numerical and experimental results

2.3 Drag reduction analysis

To investigate the effect of mass injection on drag reduction, results with and without mass injection under the same condition are compared. The comparison of local frictional coefficient along the wall is shown in Fig. 4. The resistance in solid case is almost four times more than that in porous case. We can discover impressive resistance reduction realized by mass injection.

The averaged stream wise velocity profiles of the two cases at $x=1$ m are shown in Fig. 5. The velocity without mass injection develops much faster than that with mass injection, which leads

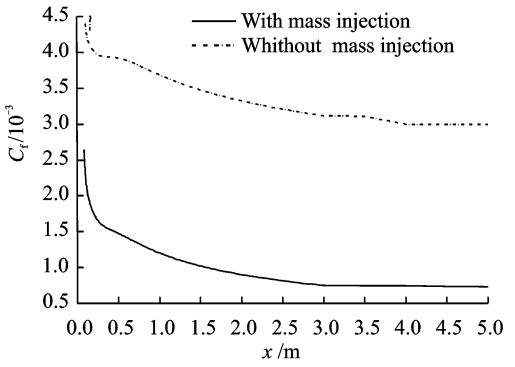

Fig. 4 Comparison of local frictional coefficient along the wall between results with and without mass injection

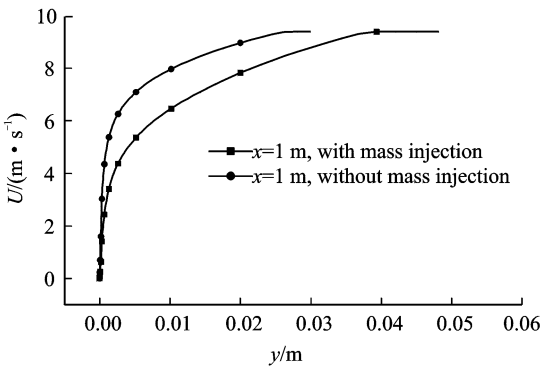

Fig. 5 Comparison of average stream wise velocity profile at x=1 m

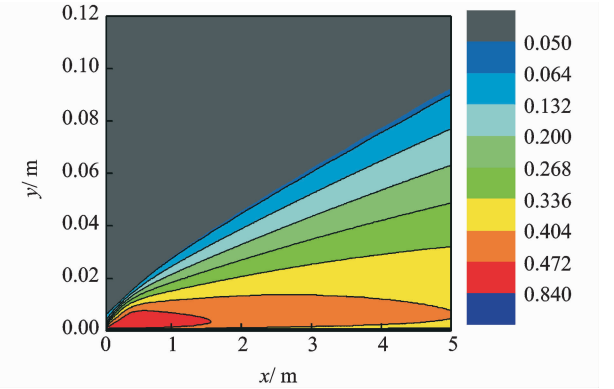

Fig. 6 Contour lines of turbulent kinetic energy in the case with mass injection

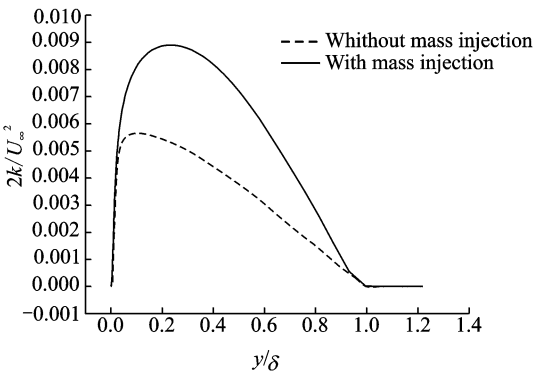

Fig. 7 Profiles of dimensionless turbulent kinetic energy at x=1 m

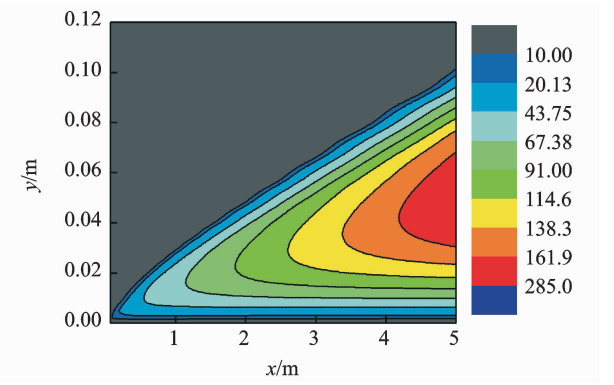

Fig. 8 Contour lines of ratio between turbulent and molecular viscous coefficients in the case with mass injection

to a higher drag value.

2.4 Turbulence quantities

Turbulent kinetic energy is directly proportional to turbulence development level, which is almost equal to zero in the zone of laminar flow. The contour lines of turbulent kinetic energy in the case with mass injection are shown in Fig. 6. According to the turbulent kinetic energy distribution, the flow structure in the boundary layer flow is developed in the middle part of the layer.

Profiles of dimensionless turbulent kinetic energy at x=1 m in the cases with/without mass injection are shown in Fig. 7. It is obvious that the flow is more turbulent in the case with mass injection.

Contour lines of ratio between eddy coefficient and molecular viscous coefficient in the case with mass injection are shown in Fig. 8. The turbulent eddy coefficient is a key value in the Reynolds-averaged numerical simulation. Greater value indicates that turbulence is better developed, which is in consistent with the above analysis.

Profiles of dimensionless turbulent eddy viscous coefficient at x=1 m in the cases with/without mass injection are compared in Fig. 9. The distance from the wall is normalized by boundary

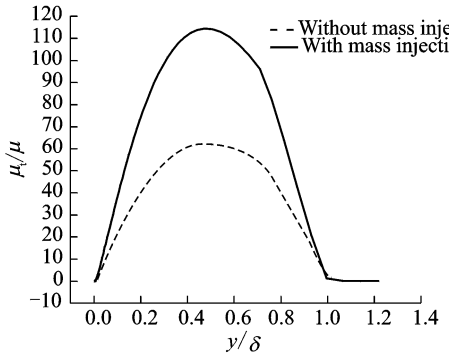

Fig. 9 Profiles of dimensionless turbulent eddy coefficient at position of $x=1$ m

layer nominal thickness. As shown in Fig. 9, eddy viscosity μ_t with mass injection is almost double the value without mass injection.

3 Conclusions

Numerical investigation is performed to study the drag reduction in two-dimensional turbulent boundary layer flows with mass injection through a porous wall. In this study, the Wilcox′s k-ω turbulence model[12] is employed. According to the comparison of numerical and experimental local frictional resistance coefficients, Wilcox′s k-ω model[12] seems to be able to predict the complex flow caused by mass injection with high precision. Numerical simulation shows that mass injection plays an active role in drag reduction by increasing the thickness of boundary layer. Meanwhile, turbulent kinetic energy and eddy viscosity are studied as well. The study also indicates that the turbulence flow is better developed with the aid of mass injection.

Acknowledgements

This work was supported by the National Natural Science Foundation of China (Nos. 51309040, 51209027, 51379025, 51379033), the Open Research Fund of State Key Laboratory of Ocean Engineering (Shanghai Jiao Tong University, No. 1402), the Young Teachers Academic Program of SWPU (No. 201499010114), the Central Financial Support of Local Key Discipline Youth Fund Project (YC319), and the Fundamental Research Fund for the Central Universities (No. DMU3132015089).

References:

[1] Gadelhak M, Bushnell D M. Status and outlook of flow separation control[R]. AIAA Paper, 1991: 91-137.

[2] Berdyugin A E, Fomin V M, Fomichev V P. Body drag control in supersonic gas flows by injection of liquid jets[J]. Journal of Applied Mechanics and Technical Physics, 1995,36(5):675-681.

[3] Quadrio M, Floryan J M, Luchini P. Effect of streamwise-periodic wall transpiration on turbulent friction drag[J]. Journal of Fluid Mechanics, 2007, 576: 425-444.

[4] Ponnaiah S. Boundary layer flow over a yawed cylinder with variable viscosity: Role of non-uniform double slot suction (injection)[J]. Int J Numer Method H, 2012, 22(3):342-356.

[5] Sun R, Szwalek J, Sirviente A I. The effects of polymer solution preparation and injection on drag reduction[J]. Journal of Fluids Engineering, Transactions of the ASME, 2005, 127(3): 536-549.

[6] Kafoussias N, Xenos M. Numerical investigation of two dimensional turbulent boundary-layer compressible flow with adverse pressure gradient and heat and mass transfer[J]. Acta Mech, 2000, 41:201-223.

[7] Akcay M, Yukselen M A. Flow of power-law fluids over a moving wedge surface with wall mass injection [J]. Archive of Applied Mechanics, 2011, 81(1):65-76.

[8] Xu S X, Huang Y. The flow with mass transfer and longitudinal velocity on the wall[J]. Acta Mechanica Sinica, 2002, 34(3):493-444.

[9] Vimalat C S, Nath G. Three dimensional laminar compressible boundary layers with large injection [J]. J Fluid Mech, 1975, 71(4):711-727.

[10] Wilcox D C. Reassessment of the scale determining equation for advanced turbulence models[J] . AIAA Journal, 1988, 26(11):1299-1310.

[11] Wilcox D C. Simulation of transition with a two equations turbulence model[J]. AIAA Journal, 1994, 32 (2): 247-255.

[12] Wilcox D C. Turbulence modeling for CFD[M]. 3rd Edition. La Canada CA:DCW Industries, Inc, 2006.

[13] Andersen P S, Kays W M, Moffat R J. The turbulent boundary layer on a porous plate: An experimental study of the fluid mechanics for adverse free-stream pressure gradients, HMT-15[R]. Stanford, USA: Dept Mech Eng, Stanford Univ,1972.

(Executive editor: Xu Chengting)